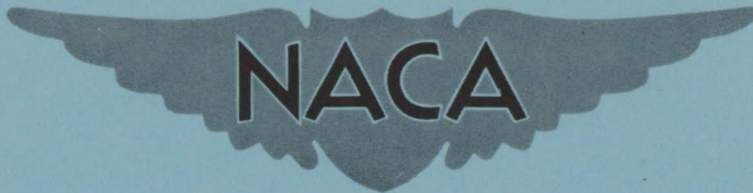


~~CONFIDENTIAL~~

Copy  
RM L52K18b

NACA RM L52K18b



# RESEARCH MEMORANDUM

PRELIMINARY RESULTS OF STABILITY AND CONTROL INVESTIGATION  
OF THE BELL X-5 RESEARCH AIRPLANE

By Thomas W. Finch and Donald W. Briggs

Langley Aeronautical Laboratory  
Langley Field, Va.

CLASSIFICATION CHANGED TO UNCLASSIFIED

AUTHORITY: NACA RESEARCH ABSTRACT NO. 97

DATE: FEBRUARY 24, 1956

WHL

CLASSIFIED DOCUMENT

Declassified

...ecting the National Defense of the United States within the meaning  
... Secs. 793 and 794, the transmission or revelation of which in any  
manner to an unauthorized person is prohibited by law.

## NATIONAL ADVISORY COMMITTEE FOR AERONAUTICS

WASHINGTON

February 11, 1953

~~CONFIDENTIAL~~

## NATIONAL ADVISORY COMMITTEE FOR AERONAUTICS

## RESEARCH MEMORANDUM

PRELIMINARY RESULTS OF STABILITY AND CONTROL INVESTIGATION  
OF THE BELL X-5 RESEARCH AIRPLANE

By Thomas W. Finch and Donald W. Briggs

## SUMMARY

During the acceptance tests of the Bell X-5 airplane, measurements of the static stability and control characteristics and horizontal-tail loads were obtained by the NACA High-Speed Flight Research Station. The results of the stability and control measurements are presented in this paper.

A change in sweep angle between  $20^\circ$  and  $59^\circ$  had a minor effect on the longitudinal trim, with a maximum change of about  $2.5^\circ$  in elevator deflection being required at a Mach number near 0.85; however, sweeping the wings produced a total stick-force change of about 40 pounds.

At low Mach numbers there was a rapid increase in stability at high normal-force coefficients for both  $20^\circ$  and  $40^\circ$  sweepback, whereas a condition of neutral stability existed for  $58^\circ$  sweepback at high normal-force coefficients. At Mach numbers near 0.8 there was an instability at normal-force coefficients above 0.5 for all sweep angles tested. In the low normal-force-coefficient range a high degree of stability resulted in high stick forces which limited the maximum load factors attainable in the demonstration flights to values under 5g for all sweep angles at a Mach number near 0.8 and an altitude of 12,000 feet.

The aileron effectiveness at  $20^\circ$  sweepback was found to be low over the Mach number range tested.

## INTRODUCTION

In order to investigate in flight the effects of large variations of sweep angle, the Bell X-5 airplane was obtained as part of the high-speed research program of the Air Force-Navy-National Advisory Committee for Aeronautics. The X-5 airplane has flight-variable sweepback between  $20^\circ$  and  $60^\circ$ .

The acceptance tests of the X-5 airplane were initiated at Edwards Air Force Base, Calif., by the Bell Aircraft Corp. with 20 flights and were completed by the Air Force with an additional 6 flights. During the acceptance tests, stability and control characteristics and horizontal-tail loads were obtained by the NACA High-Speed Flight Research Station.

The results of the horizontal-tail loads obtained during the acceptance tests have already been prepared. (See ref. 1.) The present paper presents the static stability and control data obtained at sweep angles of  $20^\circ$ ,  $40^\circ$ , and  $58^\circ$ .

## SYMBOLS

W	airplane weight, lb
S	wing area of sweep angle tested, sq ft
b	wing span, ft
$\Lambda_c/4$	sweep angle of quarter chord of wing measured between the normal to the airplane line of symmetry and the quarter-chord line, deg
$i_t$	tail incidence, deg
$\delta$	control-surface deflection, deg
$\alpha$	angle of attack, deg
F	stick force, lb
$\bar{c}$	mean aerodynamic chord, ft
p	rolling velocity, radians/sec
M	Mach number
$V_i$	indicated velocity, mph
V	true velocity, mph
q	dynamic pressure, lb/sq ft
$h_p$	pressure altitude, ft
n	normal acceleration, g units

$g$	acceleration due to gravity, ft/sec <sup>2</sup>
$C_{N_A}$	airplane normal-force coefficient, $nW/qS$
$c$	local chord, ft
$\lambda$	taper ratio
$A$	aspect ratio
$b_{c_T}$	wing span, based on equivalent tip chords, ft
$C_{N_t}$	tail normal-force coefficient, $L_t/qS_t$
$(x/\bar{c})_{WF}$	static margin of wing-fuselage combination, percent mean aerodynamic chord
$t$	time, sec
$(a.c.)_{WF}$	aerodynamic center of wing-fuselage combination, percent mean aerodynamic chord
$x$	distance from aerodynamic center of wing-fuselage combination to airplane center of gravity, positive if $(a.c.)_{WF}$ is forward of center of gravity, ft
$L_t$	aerodynamic horizontal-tail load (up tail load positive), lb
$S_t$	area of horizontal tail, sq ft
$pb/2V$	wing-tip helix angle, radians
Subscripts:	
$e$	elevator
$a$	aileron
$T$	total
$WF$	wing-fuselage combination

## DESCRIPTION OF THE AIRPLANE

The Bell X-5 airplane is a transonic research airplane incorporating a wing whose sweepback is flight-variable between 20° and 60°. It is a

single-place fighter-type airplane powered by an Allison J-35-A-17 turbojet engine. Photographs of the airplane are given in figures 1 and 2 and a three-view drawing is presented in figure 3. Some dimensions on the airplane are measured as a distance aft of fuselage station "0" shown in figure 3.

As the wing sweep angle is varied, the wing pivots about the 38.02-percent-chord point at the wing root (27.2 in. outboard of the line of symmetry) and also translates forward or rearward. Figure 4 shows the variation with wing sweep angle of the wing pivot-point location given as a measured distance to the rear of fuselage station 0. The sweep-angle limits indicated in this figure are  $20.25^{\circ}$  to  $58.7^{\circ}$  and are fixed by limit switches on the airplane which prevent interference between the wing root and the fuselage fairings. The tolerance of these limit switches is about  $\pm 0.1^{\circ}$ , and by changing the setting of the limit switches the minimum and maximum sweep-angle limits may be slightly changed. As also indicated in figure 4, the wing may be translated forward or rearward 4.5 inches from the mean translation line, except at the end points, without changing the wing sweep angle. The physical characteristics of the wing change as the wing sweep angle is varied. The variation of these characteristics with sweep angle is presented in figure 5 and table I. All wing physical characteristics were defined by standard NACA methods. It may be noted in figure 5 that the mean aerodynamic chord changes both in length and position as the wing sweep angle is changed. Therefore, positions expressed in percent of the mean aerodynamic chord at various sweep angles are not directly comparable. The center-of-gravity positions for the data shown in figures 6, 7, 10, 11, 12, 14, and 15 are given in table II.

#### INSTRUMENTATION AND ACCURACY

The following quantities were recorded on NACA internal recording instruments synchronized by a common timer:

- Vertical, longitudinal, and transverse acceleration
- Sensitive longitudinal acceleration
- Rolling angular velocity
- Pitching angular velocity and acceleration
- Yawing angular velocity and acceleration
- Airspeed and altitude
- Angle of sideslip and angle of attack
- Control positions
- Wing sweep angle
- Elevator and aileron stick forces

Strain gages were installed to record shear and bending moments on the horizontal tail.

An NACA type A-6 total-pressure tube described in reference 2 was mounted on a nose boom approximately 1.1 maximum fuselage diameters forward of the nose of the airplane. The position error of the tube was calibrated by the "fly-by" method up to  $M = 0.70$  and above  $M = 0.70$  by the radar-phototheodolite method presented in reference 3. The estimated error in Mach number is about  $\pm 0.01$ .

With an estimated error of  $\pm 100$  pounds in the weight determination and an estimated error of  $\pm 0.02g$  in normal acceleration in conjunction with the estimated Mach number error, the maximum error in the determination of airplane normal-force coefficient would be about  $\pm 0.03$ .

## TESTS

The flight data obtained during the acceptance tests of the X-5 airplane covered an altitude range of 10,000 feet to 35,000 feet and a weight range of 8,350 pounds to 9,650 pounds. The tests were conducted at sweep angles of  $20^\circ$ ,  $40^\circ$ , and  $58^\circ$  for the mean translation position only and consisted of the following: (a) Wing-sweep-angle changes at about  $M = 0.54$  and  $0.85$ ; (b)  $1g$  stalls at sweep angles of  $20^\circ$ ,  $40^\circ$ , and  $58^\circ$ ; (c) accelerated turns at 30,000 feet ( $M = 0.84$ ) and at 12,000 feet ( $M = 0.83$ ) for sweep angles of  $20^\circ$ ,  $40^\circ$ , and  $58^\circ$ ; and (d) aileron rolls at  $20^\circ$  sweep for a Mach number range of  $0.54$  to  $0.81$ .

## RESULTS AND DISCUSSION

### Longitudinal Stability and Control

Effect of sweep on longitudinal trim.- Figure 6 presents time histories of sweep-angle changes from  $20^\circ$  to  $57^\circ$  and from  $57^\circ$  to  $21^\circ$  at a Mach number of about  $0.54$  and at an altitude of 20,000 feet. A time history of a continuous sweep-angle change from  $20^\circ$  to  $59^\circ$  to  $20^\circ$  at a Mach number of about  $0.85$  and an altitude of about 20,000 feet is presented in figure 7. The effect of sweep on longitudinal trim is presented in figure 8 as the variation of elevator position required for trim with angle of sweep. These data were taken from figures 6 and 7 and indicate that at the low Mach number the elevator required for trim gradually increases from  $1^\circ$  up at  $20^\circ$  sweepback to about  $2.5^\circ$  up at  $40^\circ$  sweepback and then decreases to about  $2^\circ$  up at  $58^\circ$  sweepback. The elevator required for trim was determined by a summation of the change in elevator required for each individual sweep-angle change and would, therefore, generally apply for the initial tail-incidence setting of  $-3^\circ$ . The change in trim is accompanied by a 12-pound change in stick force. At the higher Mach number the trim is approximately constant at  $1^\circ$  up

elevator from  $20^\circ$  to  $30^\circ$  sweepback and then gradually decreases to about  $1.5^\circ$  down elevator at  $60^\circ$  sweepback. Although the change in elevator deflection required for trim with sweep is small at a Mach number of 0.85, there is a change in elevator stick force of about 40 pounds. (See fig. 7.) The probable causes for the scatter between data taken with increasing and decreasing sweep angle were changes in Mach number, altitude, and normal acceleration during the sweep-angle change.

The effect of sweepback on longitudinal trim may also be seen in figure 9 where the variations of stabilizer deflection required for trim with indicated airspeed for sweep angles of  $20^\circ$ ,  $40^\circ$ , and  $58^\circ$  are shown. These trim data were obtained with zero elevator stick force and with the elevator deflection varying from  $0^\circ$  to  $1^\circ$  up. The variation of stabilizer deflection required for trim is stable for all sweep angles, with negative stabilizer deflection decreasing with increasing airspeed. Although the data were obtained over an altitude range of about 10,000 to 45,000 feet, insufficient test points are available to show the effects of altitude on trim. Data presented in reference 1 indicate that the maximum downward tail load occurs at approximately  $36^\circ$  sweepback; however, insufficient information is available to determine the sweep angle requiring maximum trim.

Stall-approach data.- Stall-approach data for the clean configuration at  $20^\circ$ ,  $40^\circ$ , and  $58^\circ$  sweepback are presented in figure 10. Horizontal-tail-load information is also presented as the coefficient  $C_{N_t}$ , to show the variation of wing-fuselage stability with lift. Because of high angular pitching accelerations and buffet accelerations, the accuracy of reading the tail loads was low; therefore, the data above  $\alpha = 18.5^\circ$  at  $40^\circ$  sweepback have been omitted. A measure of the stability of the airplane is also shown in figure 10 as a variation of elevator position with airplane normal-force coefficient. There is an abrupt increase in stability for  $20^\circ$  sweepback at  $C_{N_A} = 0.7$  and at  $C_{N_A} = 0.8$  for  $40^\circ$  sweepback. However, there is a trend toward neutral stability at  $40^\circ$  sweepback prior to the abrupt increase in stability. At  $58^\circ$  sweepback a condition of neutral stability exists above  $C_{N_A} = 0.7$ . The measured value of the slope of the airplane normal-force-coefficient curve with angle of attack (fig. 10) in the linear portion is about 0.058 at  $20^\circ$  sweepback and about 0.045 at  $40^\circ$  and  $58^\circ$  sweepback. There was some sticking of the angle-of-attack vane which made the angle of attack measured for the  $40^\circ$  sweepback data questionable; therefore, the value of 0.045 measured as the slope of the airplane normal-force-coefficient curve with angle of attack may be in error.

As noted by the pilot, the stall approach and recovery were conventional at  $20^\circ$  and  $40^\circ$  sweepback with no unusual tendency to pitch up, but at  $58^\circ$  sweepback a mild longitudinal instability was observed. The

pilot reported a stall warning in the form of buffeting at indicated airspeeds of about 180, 175, and 180 miles per hour for sweep angles of  $20^\circ$ ,  $40^\circ$ , and  $58^\circ$ . A buffet-intensity rise was noted on the records at similar indicated airspeeds.

Since the maneuvers were terminated prior to a complete stall, the present data do not fully describe the stalling characteristics in the clean configuration.

Accelerated maneuvers.- Data from accelerated turns performed at  $20^\circ$ ,  $40^\circ$ , and  $58^\circ$  sweepback at Mach numbers near 0.84 and an altitude of 30,000 feet are presented in figure 11. An instability at the higher normal-force coefficients for all sweep angles was indicated by a change from a positive to a negative slope of the curve of  $\delta_e$  against  $C_{NA}$ . At  $20^\circ$  sweepback this decrease in stability occurs at  $C_{NA} = 0.5$  at a Mach number of 0.82. An abrupt decrease in stability occurs at  $C_{NA} = 0.5$  and a Mach number of about 0.84 at  $40^\circ$  sweepback and at  $C_{NA} = 0.56$  at  $58^\circ$  sweepback following a decrease in Mach number to about 0.80. The value of the measured slope of  $C_{NA}/\alpha$  decreased from about 0.095 at  $20^\circ$  sweepback to 0.05 at  $58^\circ$  sweepback. Angle-of-attack measurements were not available to determine the value of the slope at  $40^\circ$  sweepback. Most of the decrease in the slope  $C_{NA}/\alpha$  was caused by the decrease in aspect ratio from 6.1 to 2.2 associated with a sweep-angle change from  $20^\circ$  to  $58^\circ$ . The elevator-control-force gradient measured from the variation of elevator control force with normal acceleration is high, increasing from about 33 pounds per g at  $20^\circ$  sweepback to about 38 pounds per g at  $40^\circ$  and  $58^\circ$  sweepback (fig. 11).

It was required in the acceptance program that the airplane be demonstrated to a load factor of 5.86g at a Mach number of 0.8 and an altitude of 12,000 feet. Figure 12 presents the data obtained from the accelerated maneuvers performed at sweep angles of  $20^\circ$ ,  $40^\circ$ , and  $58^\circ$ . Because of the high stick forces resulting from the high stability inherent in the airplane, as noted in figure 12 where elevator control force is presented as a variation with normal acceleration, the maximum load factors the pilot could attain were 3.9g, 4.0g, and 4.9g for sweep angles of  $20^\circ$ ,  $40^\circ$ , and  $58^\circ$ , respectively. In comparison with the data obtained at 30,000 feet, the slopes  $d\delta_e/dC_{NA}$  obtained at 12,000 feet indicate an increase in stability. However, the tail loads show no change in stability of the wing-fuselage combination, indicating that the change in apparent stability may be caused by deformation of the tail and the change in the curvature of the flight path with altitude for a constant  $C_{NA}$ .

The high degree of stability at low normal-force coefficients as determined by the measured slopes of  $\delta_e$  against  $C_{NA}$  in figure 11



may be partially explained by figure 13 in which the position of the aerodynamic center of the wing-fuselage combination and airplane center-of-gravity position in percent mean aerodynamic chord are presented for 3 wing sweep angles. These data were obtained from reference 1. Although the center-of-gravity position changes from about 23 percent to 45 percent mean aerodynamic chord as the sweepback changes from  $20^\circ$  to  $59^\circ$ , the wing-fuselage combination remains almost neutrally stable throughout the sweep range as indicated by the variation of the wing-fuselage static margin  $(x/\bar{c})_{WF}$  with sweep angle as shown in figure 13. The large horizontal-tail contribution to stability is a result of a large tail needed to trim the airplane in the power-on landing configuration (slats out, flaps down, and gear down). Therefore, the very high stability of the airplane is caused by the large horizontal-tail contribution with a minor contribution from the wing-fuselage combination.

### Lateral Control

A limited amount of aileron-effectiveness data from rudder-fixed rolls was obtained at 25,000 feet for Mach numbers of about 0.54, 0.72, and 0.81 at  $20^\circ$  sweepback. The maximum total aileron deflections attained were determined by the maximum stick force the pilot could exert.

Aileron effectiveness as evaluated in terms of the variation of wing-tip helix angle  $pb/2V$  and the change in aileron stick force with total aileron deflection is presented in figure 14. At Mach numbers of 0.54 and 0.72,  $pb/2V$  is approximately linear with total aileron deflection. At  $M = 0.81$ ,  $pb/2V$  is nearly linear with total aileron deflection up to  $\delta_{aT} = \pm 10^\circ$  and becomes nonlinear above these deflections. The stick force for about half-deflection rolls varied from about 30 pounds at  $M = 0.54$  to about 45 pounds at  $M = 0.81$ .

The wing-tip helix angle per degree of total aileron deflection is presented as a function of Mach number in figure 15. The slopes over a total aileron deflection of  $\pm 10^\circ$  were taken from figure 14. These values are appreciably lower than those predicted in reference 4.

### CONCLUSIONS

From the results obtained during the acceptance tests of the Bell X-5 airplane it may be concluded that:

1. A change in sweep angle between  $20^\circ$  and  $59^\circ$  at Mach numbers of 0.54 and 0.85 had only a small effect on longitudinal trim with maximum

change of  $2.5^{\circ}$  in elevator deflection required at a Mach number of 0.85. However, sweeping the wing produced a total stick-force change of about 40 pounds at a Mach number of 0.85.

2. In stall approaches at low Mach numbers the stability increased rapidly at higher normal-force coefficients for both  $20^{\circ}$  and  $40^{\circ}$  sweepback, but at  $58^{\circ}$  sweepback a condition of neutral stability existed at normal-force coefficients above 0.7.

3. At Mach numbers near 0.80 there was an instability at normal-force coefficients above 0.5 for all sweep angles.

4. The airplane was very stable longitudinally at lift coefficients up to about 0.3, resulting in maneuvering stick-force gradients in excess of 33 pounds per g for all sweep angles. As a result of this high stability it was not possible to obtain more than 4.9g at 12,000 feet and a Mach number near 0.80.

5. The aileron effectiveness at  $20^{\circ}$  sweepback was low over the range of Mach numbers from 0.54 to 0.81.

Langley Aeronautical Laboratory,  
National Advisory Committee for Aeronautics,  
Langley Field, Va

## REFERENCES

1. Rogers, John T., and Dunn, Angel H.: Preliminary Results of Horizontal Tail-Load Measurements of the Bell X-5 Research Airplane. NACA RM L52G14, 1952.
2. Gracey, William, Letko, William, and Russell, Walter R.: Wind-Tunnel Investigation of a Number of Total-Pressure Tubes at High Angles of Attack. Subsonic Speeds. NACA TN 2331, 1951. (Supersedes NACA RM L50G19.)
3. Zalovcik, John A.: A Radar Method of Calibrating Airspeed Installations on Airplanes in Maneuvers at High Altitudes and at Transonic and Supersonic Speeds. NACA Rep. 985, 1950. (Supersedes NACA TN 1979.)
4. O'Malley, J., DiFranco, D., et al.: Static Stability and Control Analysis of the Bell Model 60 (MX1095; X-5) Research Airplane. Rep. No. 60-978-005, Bell Aircraft Corp., Apr. 24, 1950.

TABLE I.- PHYSICAL CHARACTERISTICS OF BELL X-5 AIRPLANE

Airplane:

Weight, lb:

Full fuel . . . . .	9,960
Less fuel . . . . .	7,850

Power plant:

Axial-flow turbojet engine . . . . .	J-35-A-17
Guaranteed rated thrust at 7,800 rpm and static sea-level conditions, lb . . . . .	4,900

Moments of inertia (clean configuration - full fuel),  
slug-ft<sup>2</sup>:

Sweep angle at 0.25 local chord, deg . . . . .	20	45	59
About X-axis . . . . .		Not available	
About Y-axis . . . . .	9,450	9,720	9,810
About Z-axis . . . . .		Not available	

Center-of-gravity position, percent M.A.C.:

Sweep angle, deg . . . . .	20	45	59
Full fuel . . . . .	24.7	32.0	45.6
Less fuel . . . . .	26.3	33.0	46.2
Over-all height, ft . . . . .			12.2
Over-all length, ft . . . . .			33.6

Wing:

Airfoil section (perpendicular to 38.02-percent-chord line):

Pivot point . . . . .	NACA 64 <sub>(10)</sub> A011
Tip . . . . .	NACA 64 <sub>(08)</sub> A008.28

Sweep angle at 0.25 local chord, deg . . . . .	20
Area, sq ft . . . . .	167.0
Span, ft . . . . .	31.9
Span between equivalent tips, ft . . . . .	30.9
Aspect ratio . . . . .	6.09
Taper ratio . . . . .	0.435
Mean aerodynamic chord, ft . . . . .	5.61

Location of leading edge of mean aerodynamic chord,

fuselage station . . . . .	139.9
Incidence, root chord, deg . . . . .	0
Dihedral, deg . . . . .	0
Geometric twist, deg . . . . .	0

Wing flaps (split):

Area, sq ft . . . . .	15.9
Span, parallel to hinge center line, ft . . . . .	6.53
Chord, parallel to line of symmetry at 20° sweepback, in.:	
Root . . . . .	30.8
Tip . . . . .	19.2
Travel, deg . . . . .	60



TABLE I.- PHYSICAL CHARACTERISTICS OF BELL X-5 AIRPLANE - Continued

Slats (leading edge divided):	
Area, sq ft . . . . .	14.6
Span, parallel to leading edge, ft . . . . .	10.3
Chord, perpendicular to leading edge, in.:	
Root . . . . .	11.1
Tip . . . . .	6.6
Travel, percent wing chord:	
Forward . . . . .	10
Down . . . . .	5
Aileron (0.45c <sub>a</sub> internal-seal pressure balance):	
Area (each aileron behind hinge line), sq ft . . . . .	3.62
Span parallel to hinge center line, ft . . . . .	5.15
Travel, deg . . . . .	±15
Chord, percent wing chord . . . . .	19.7
Moment area rearward of hinge line (total), in. <sup>3</sup> . . . . .	4,380
Horizontal tail:	
Airfoil section (parallel to fuselage center line) . . .	NACA 65A006
Area, sq ft . . . . .	31.5
Span, ft . . . . .	9.56
Aspect ratio . . . . .	2.9
Sweep angle at 0.25-percent chord, deg . . . . .	45
Mean aerodynamic chord, in. . . . .	42.8
Position of 0.25 mean aerodynamic chord, fuselage station . . .	355.6
Stabilizer travel, (power-actuated), deg:	
Leading edge up . . . . .	4.5
Leading edge down . . . . .	7.5
Elevator (0.208c <sub>e</sub> overhang balance, 31.5 percent span):	
Area rearward of hinge line, sq ft . . . . .	6.9
Travel from stabilizer, deg:	
Up . . . . .	25
Down . . . . .	20
Chord, percent horizontal tail chord . . . . .	30
Moment area rearward of hinge line (total), in. <sup>3</sup> . . . . .	4,200
Vertical tail:	
Airfoil section (parallel to rear fuselage center line) . . . . .	NACA 65A006
Area, sq ft . . . . .	29.5
Span, perpendicular to rear fuselage center line, ft . . . . .	6.25
Aspect ratio . . . . .	1.32
Sweep angle of leading edge, deg . . . . .	43
Fin:	
Area, sq ft . . . . .	24.8



TABLE I.- PHYSICAL CHARACTERISTICS OF BELL X-5 AIRPLANE - Concluded

Rudder (0.231c<sub>r</sub> overhang balance, 26.3 percent span):

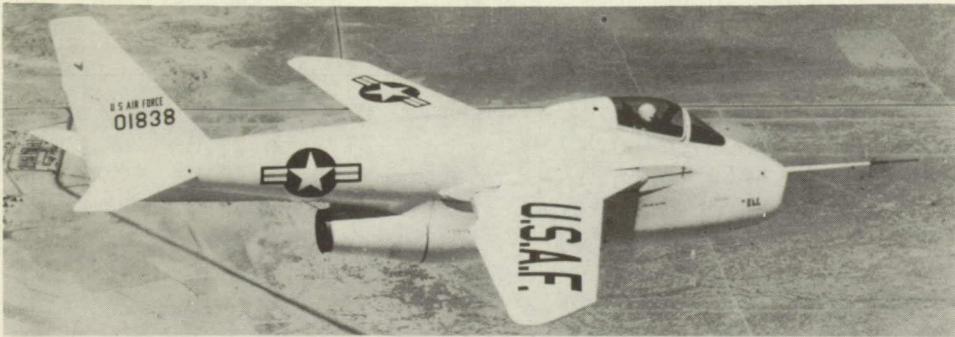
Area rearward hinge line, sq ft . . . . .	4.7
Span, ft . . . . .	4.43
Travel, deg . . . . .	±35
Chord, percent horizontal tail chord . . . . .	22.7
Moment area rearward of hinge line, in. <sup>3</sup> . . . . .	3,585



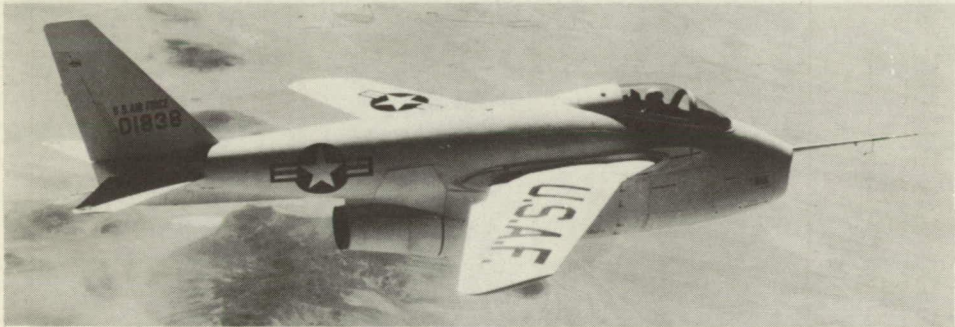
TABLE II.- CENTER-OF-GRAVITY POSITIONS

Figure	$\Lambda_c/4$ , deg	Center-of-gravity position, percent M.A.C.
6(a)	20.0 to 30.6	22.9 to 23.2
6(b)	30.6 to 40.4	23.2 to 27.0
6(c)	40.4 to 45.0	27.0 to 30.5
6(d)	45.0 to 50.0	30.5 to 34.1
6(e)	50.0 to 54.5	34.1 to 39.3
6(f)	54.5 to 57.4	39.3 to 42.4
6(g)	57.4 to 21.0	42.4 to 23.0
7	20	23.6
	59	44.6
	20	23.6
10(a)	20	24.0
10(b)	40	28.0
10(c)	58	43.6
10(d)	20	24.0
10(e)	40	28.0
10(f)	58	43.6
11(a)	20	23.0
11(b)	40	28.0
11(c)	58	43.6
11(d)	20	23.0
11(e)	40	28.0
11(f)	58	43.6
12(a)	20	24.2
12(b)	40	28.2
12(c)	58	43.7
12(d)	20	24.2
12(e)	40	28.2
12(f)	58	43.7
14	20	23.0
15	20	23.0





(a) 20° sweepback.



(b) 45° sweepback.



(c) 60° sweepback.

Figure 1.- Photographs of the Bell X-5 airplane in flight.

NACA  
L-77039





Figure 2.- Photograph of Bell X-5 airplane in landing configuration.

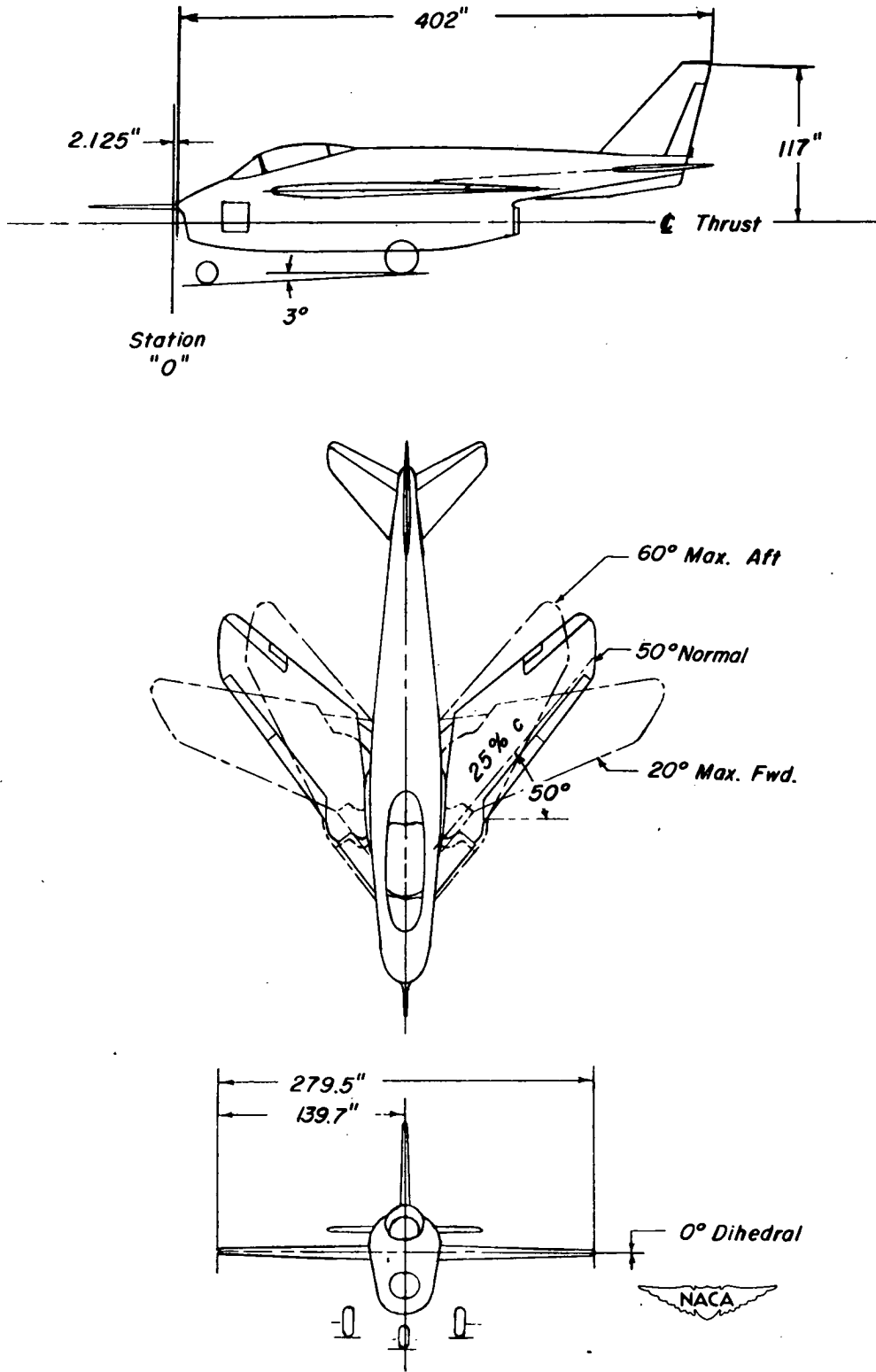


Figure 3.- Three-view drawing of the X-5 airplane.

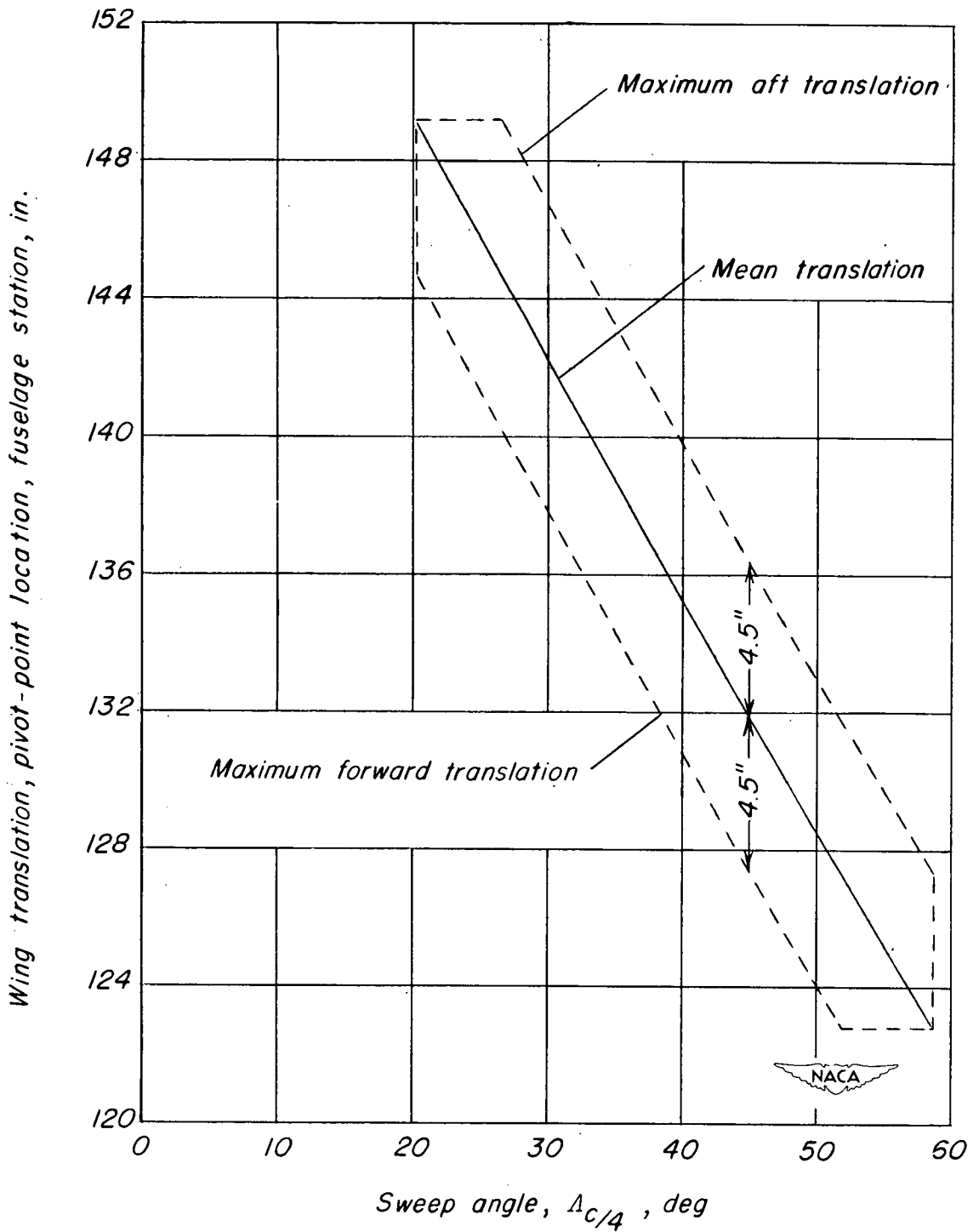


Figure 4.- Wing pivot-point location plotted against wing sweep angle. X-5 airplane.

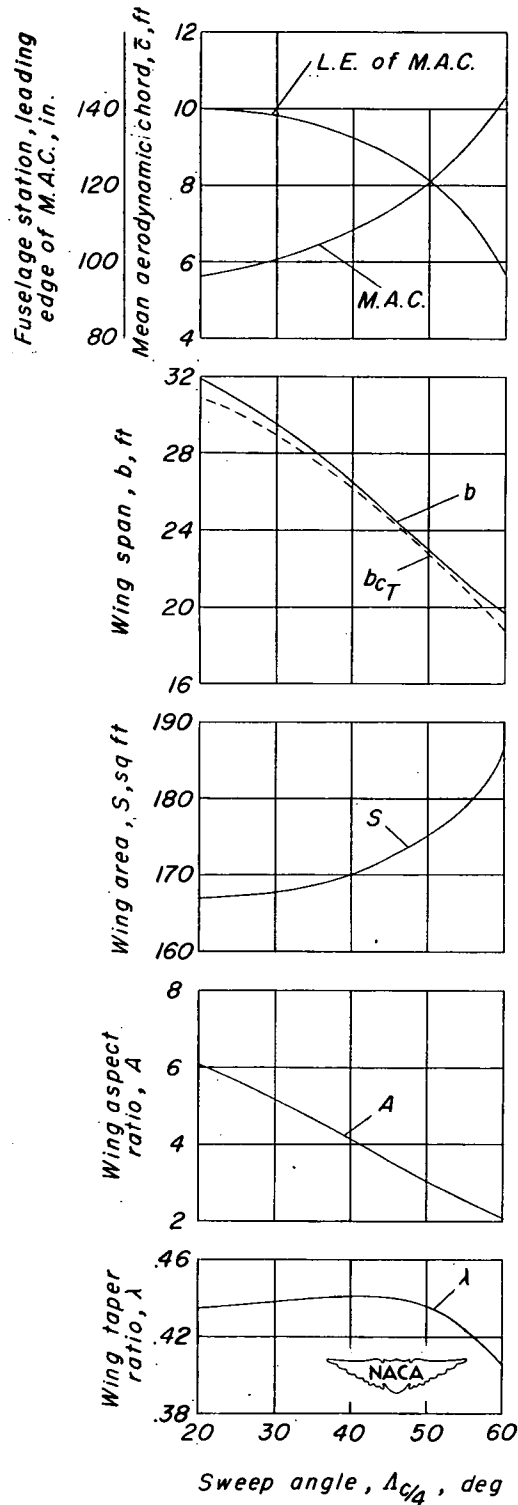


Figure 5.- Dimensional characteristics of X-5 airplane plotted against wing sweep angle.

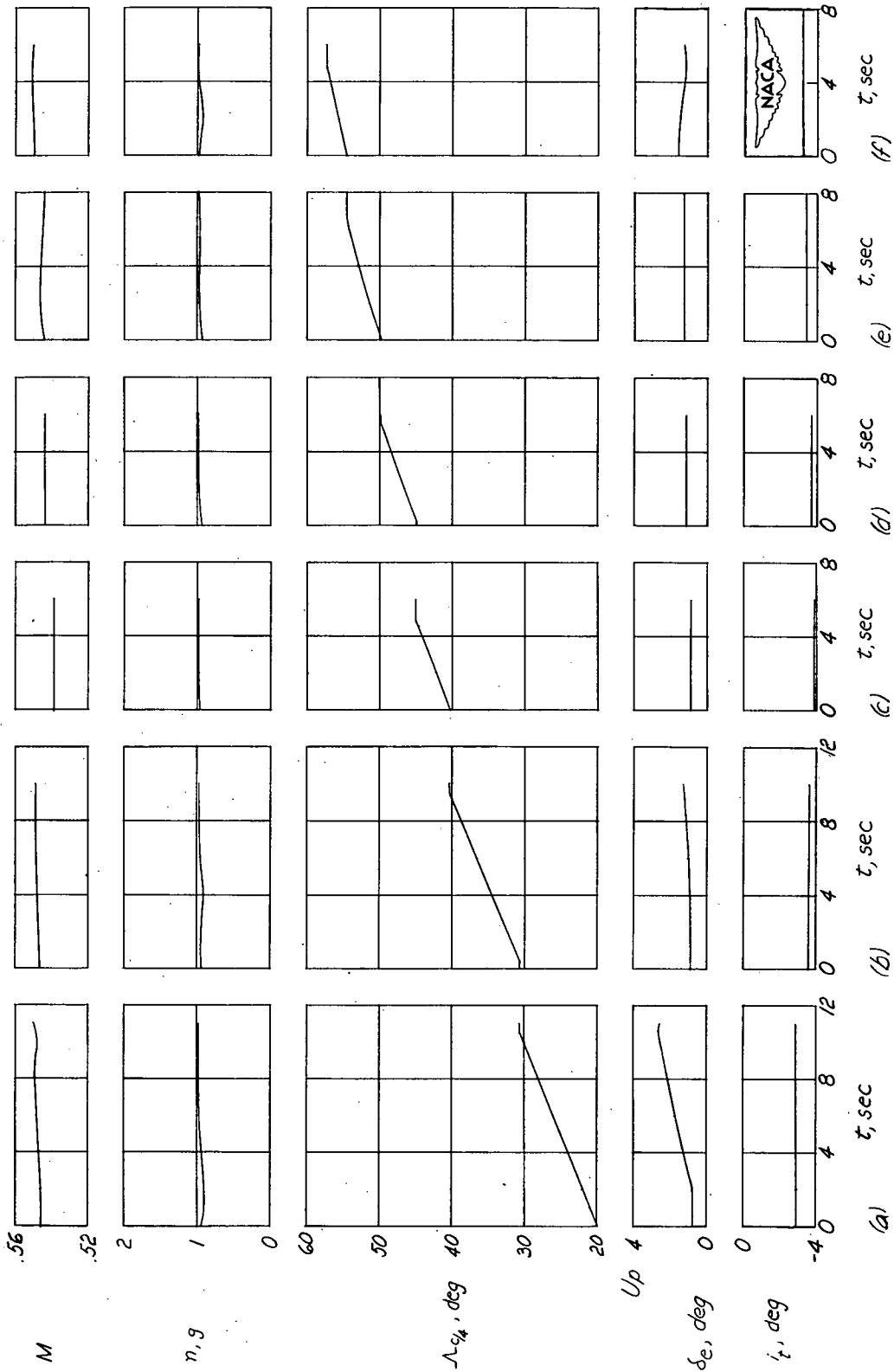


Figure 6.- Time history of wing-sweep change in the clean configuration near  $M = 0.54$ .  $h_p = 20,000$  feet.

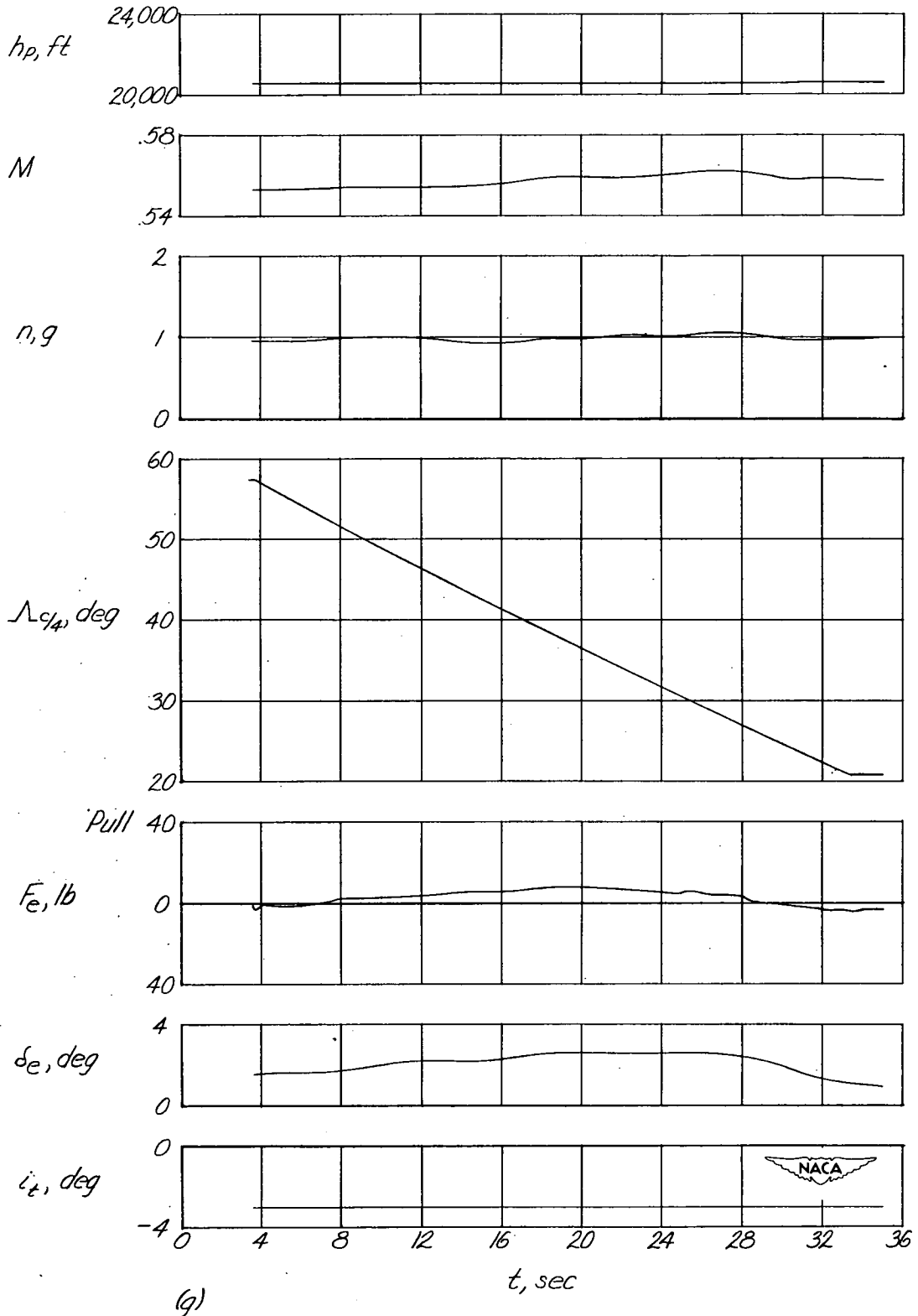


Figure 6.- Concluded.

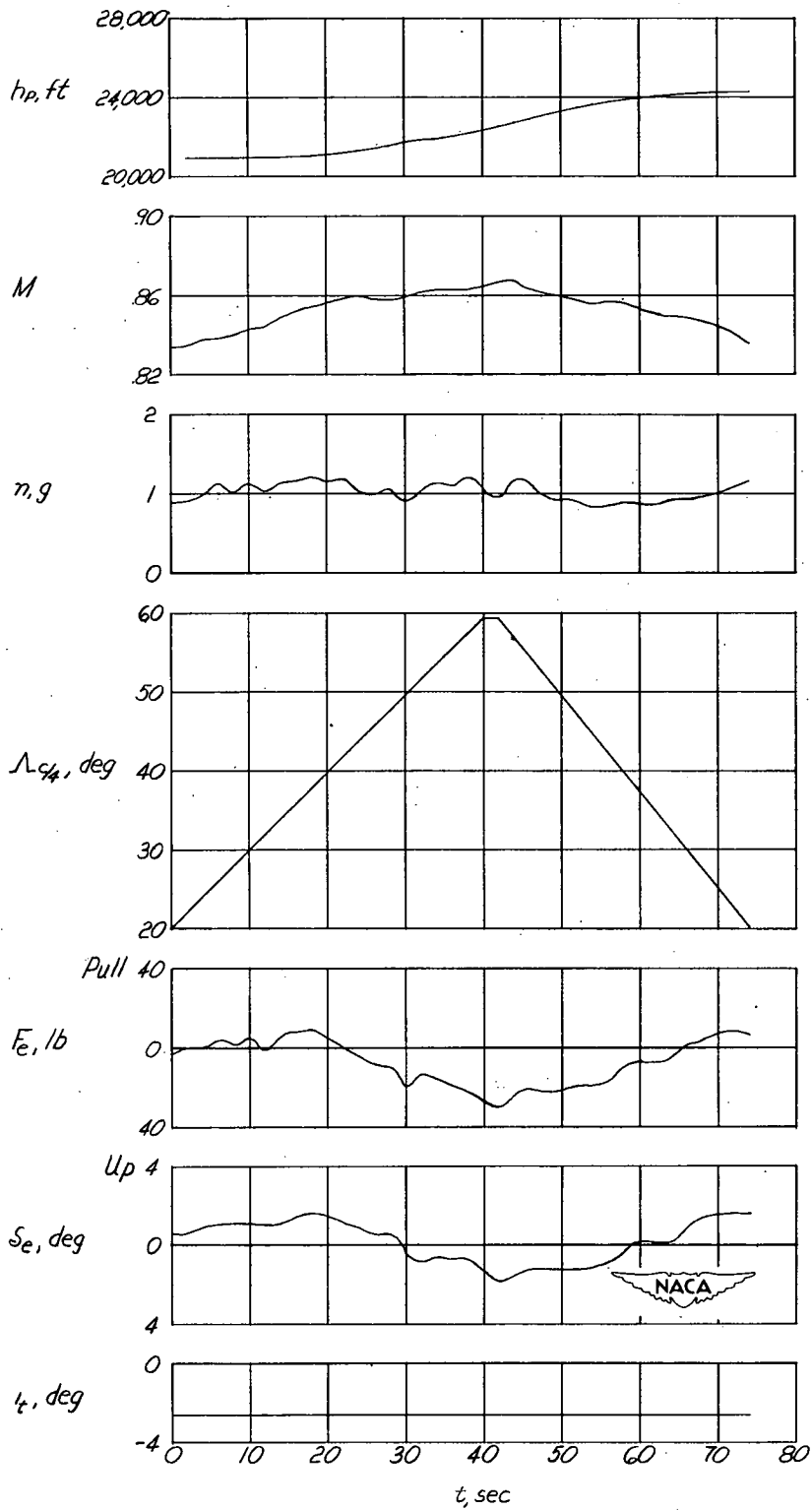


Figure 7.- Time history of a continuous wing-sweep change in the clean configuration near  $M = 0.85$ .

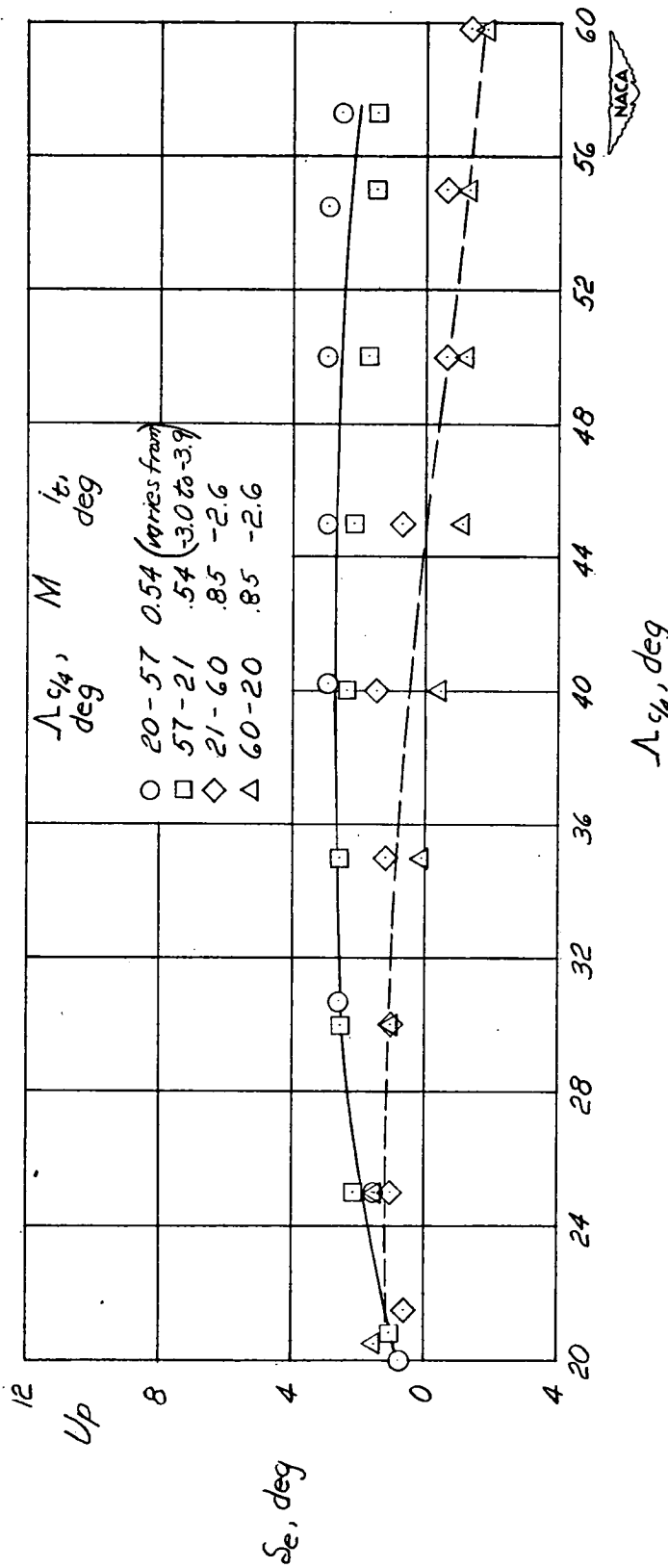


Figure 8.- Variation of elevator deflection required for trim with angle of sweep at Mach number of 0.54 and 0.85.  $h_p \approx 20,000$  feet.



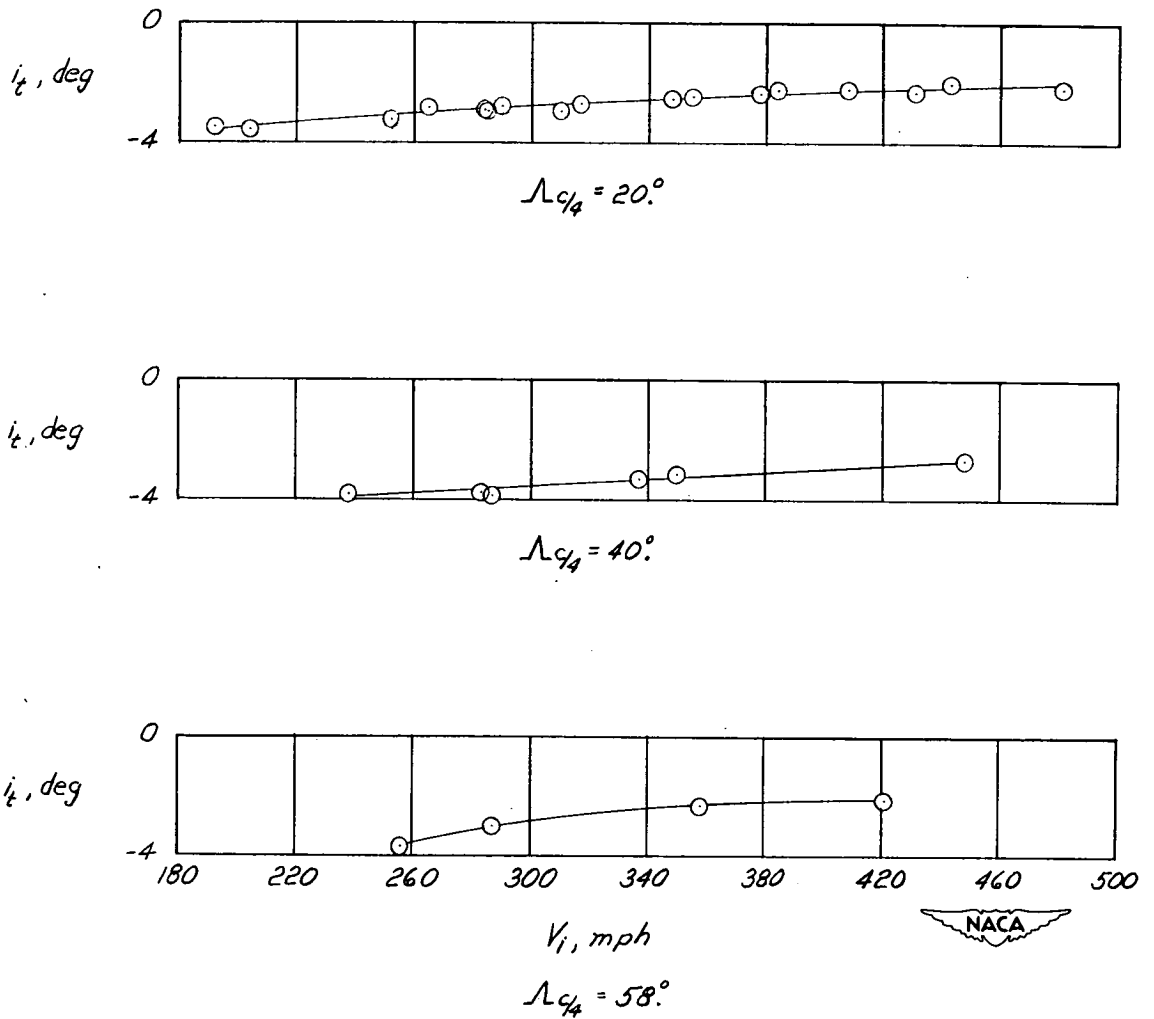


Figure 9.- Variation of stabilizer deflection required for trim with indicated velocity for sweep angles of  $20^\circ$ ,  $40^\circ$ , and  $58^\circ$ .  $\delta_e \approx 0^\circ$ .

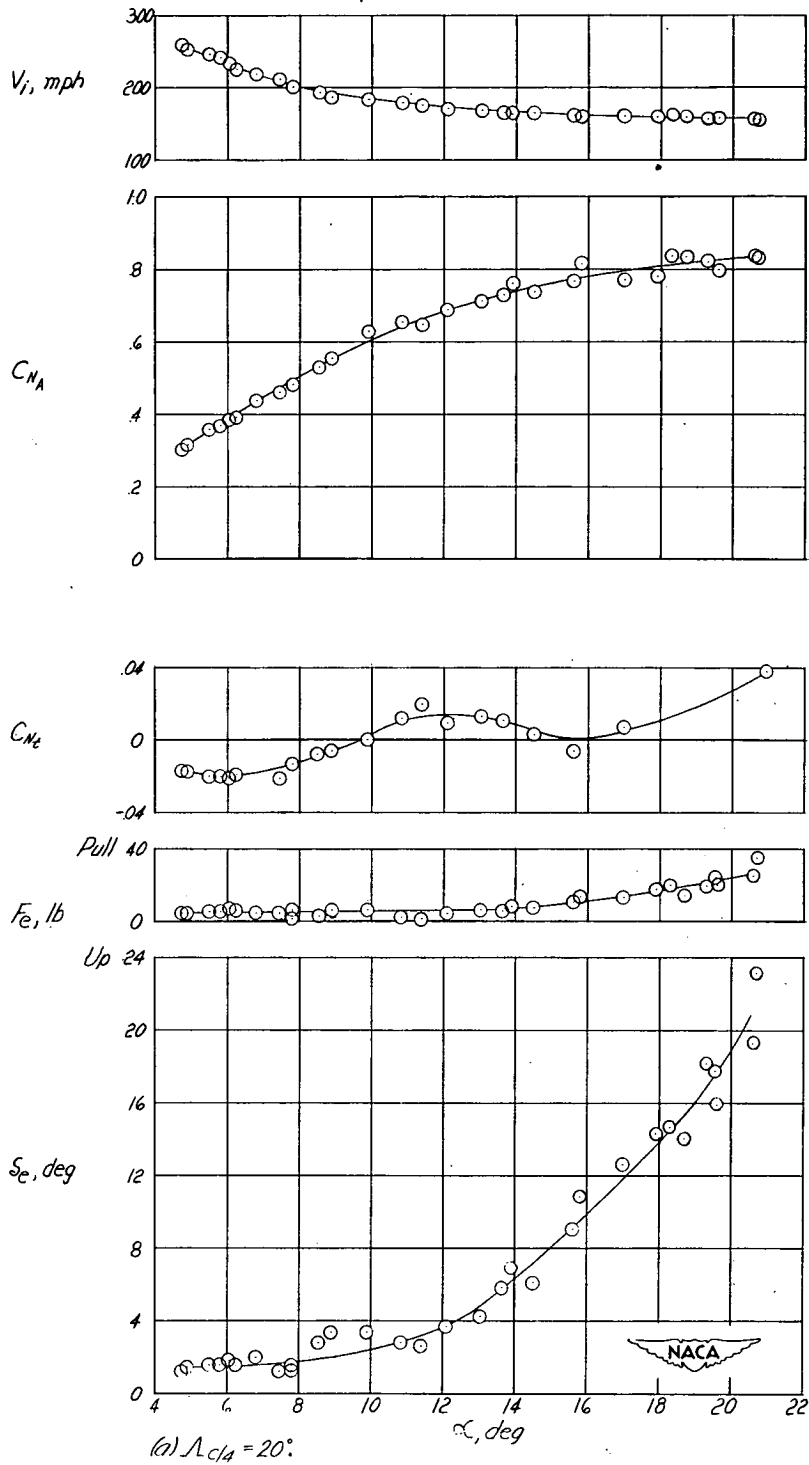


Figure 10.- Variation of measured quantities obtained during stall approaches in the clean configuration at 20,000 feet for sweep angles of  $20^\circ$ ,  $40^\circ$ , and  $58^\circ$ .

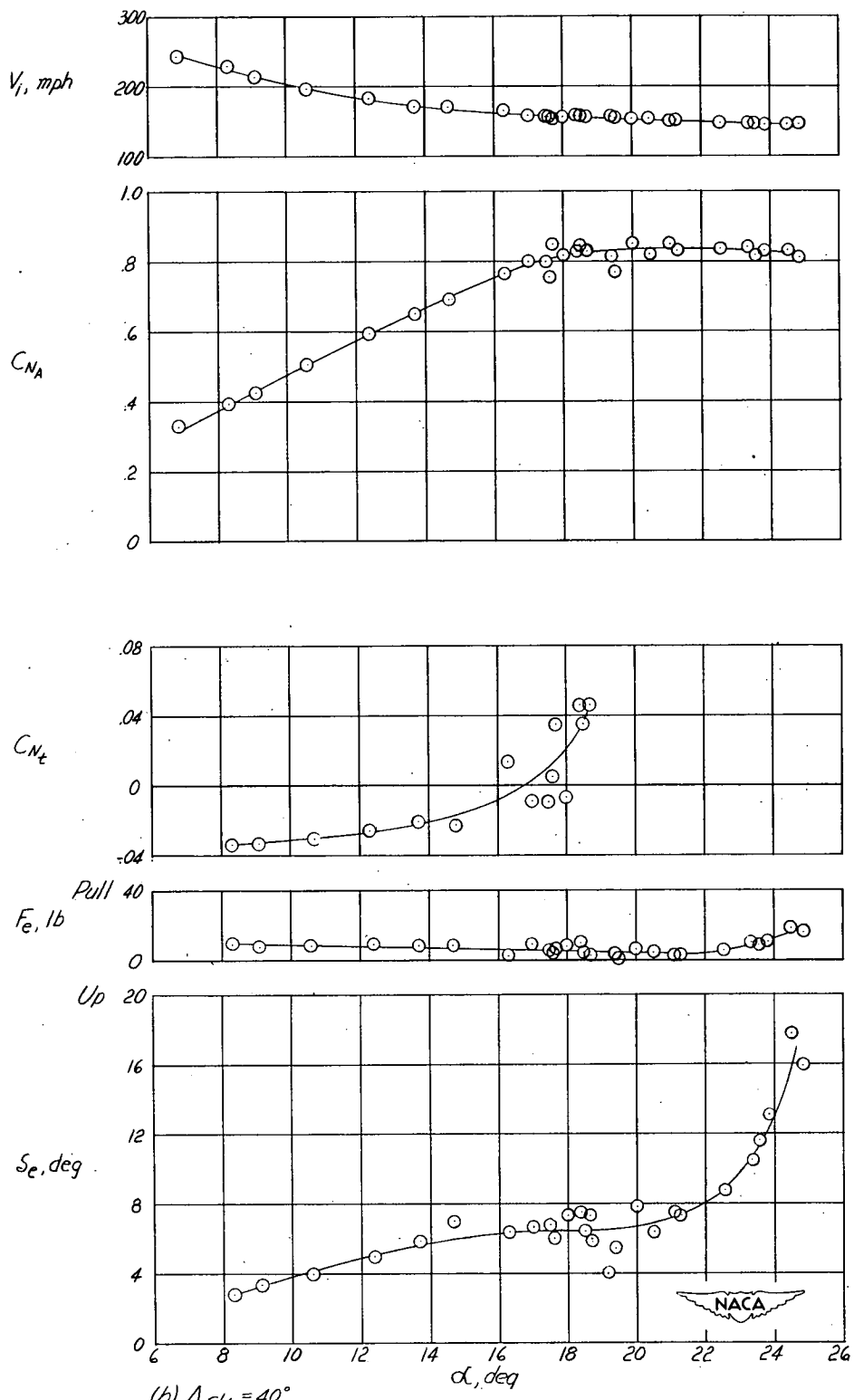


Figure 10.- Continued.

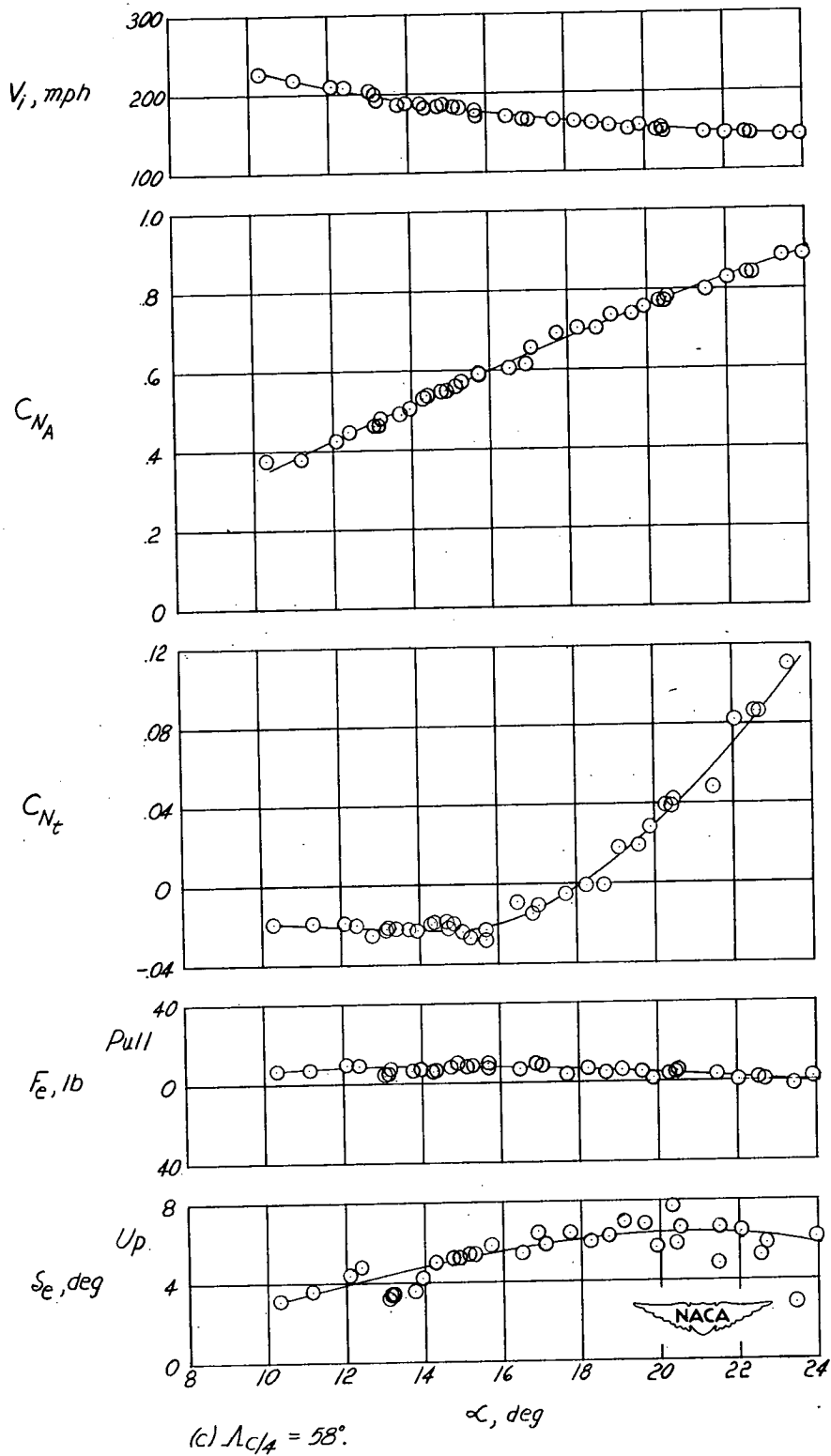


Figure 10.- Continued.

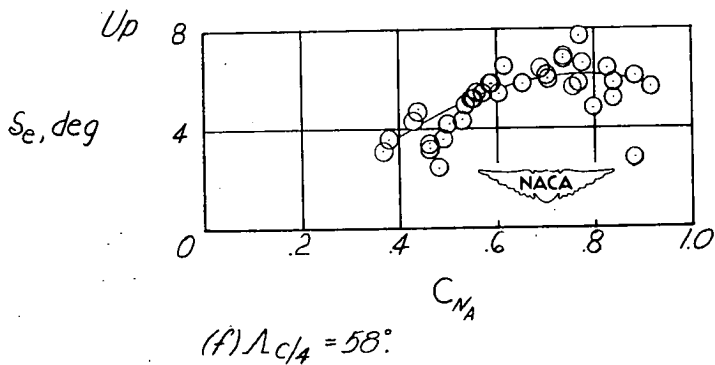
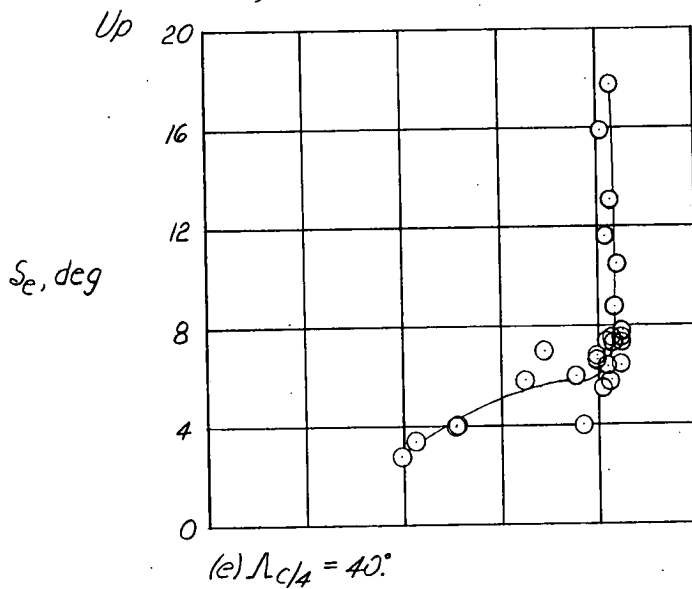
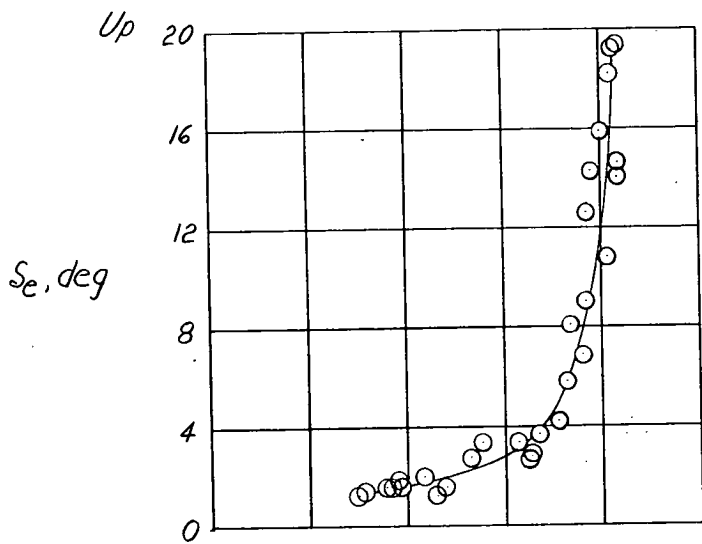


Figure 10.- Concluded.

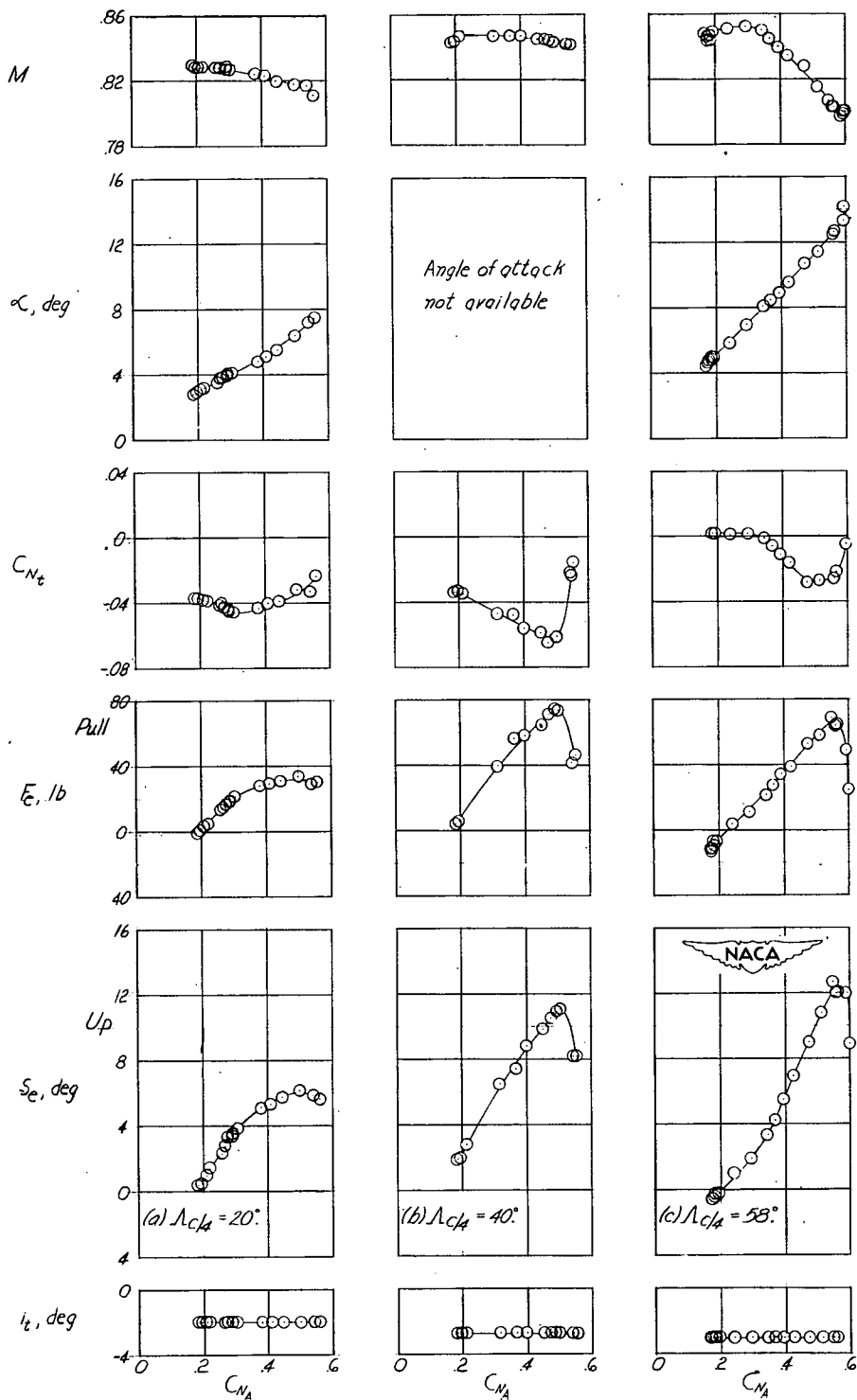


Figure 11.- Variation of measured quantities obtained during accelerated flight in clean configuration near a Mach number of 0.84 for sweep angles of  $20^\circ$ ,  $40^\circ$ , and  $58^\circ$ .  $h_p = 30,000$  feet.

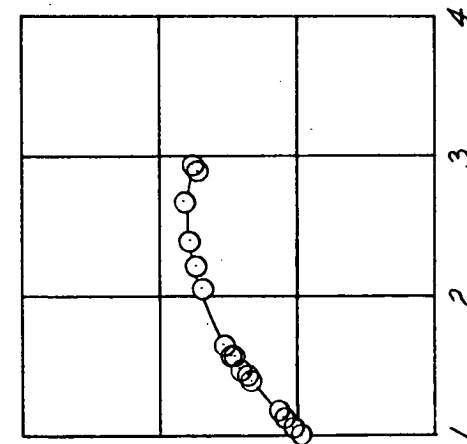
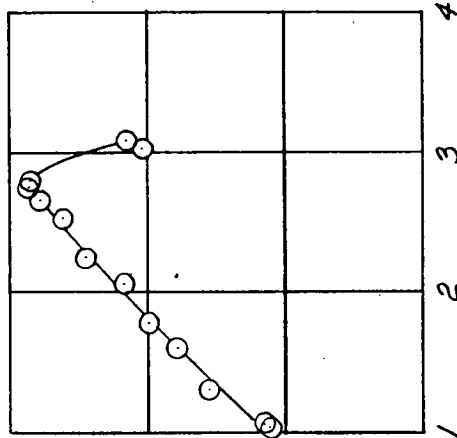
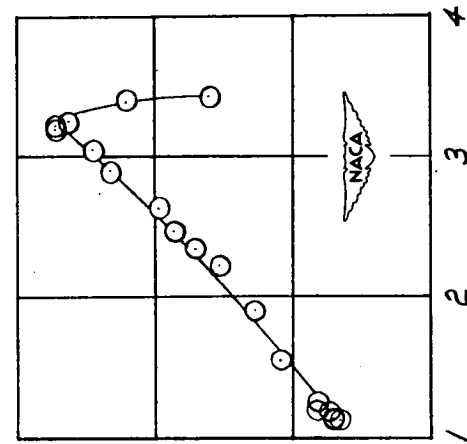


Figure 11.- Concluded.

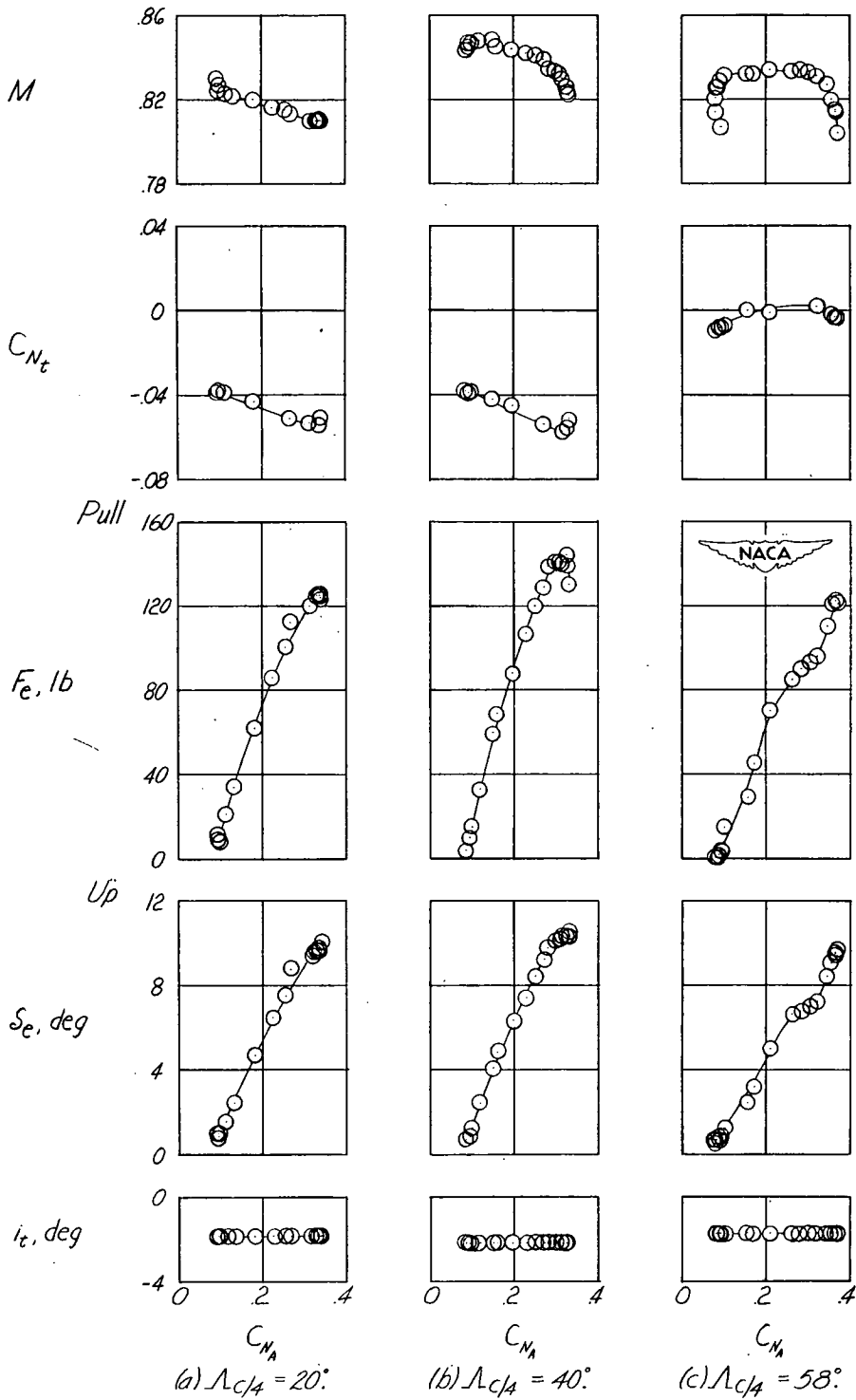


Figure 12.- Variation of measured quantities obtained during accelerated flight in the clean configuration near a Mach number of 0.83 for sweep angles of  $20^\circ$ ,  $40^\circ$ , and  $58^\circ$ .  $h_p = 12,000$  feet.



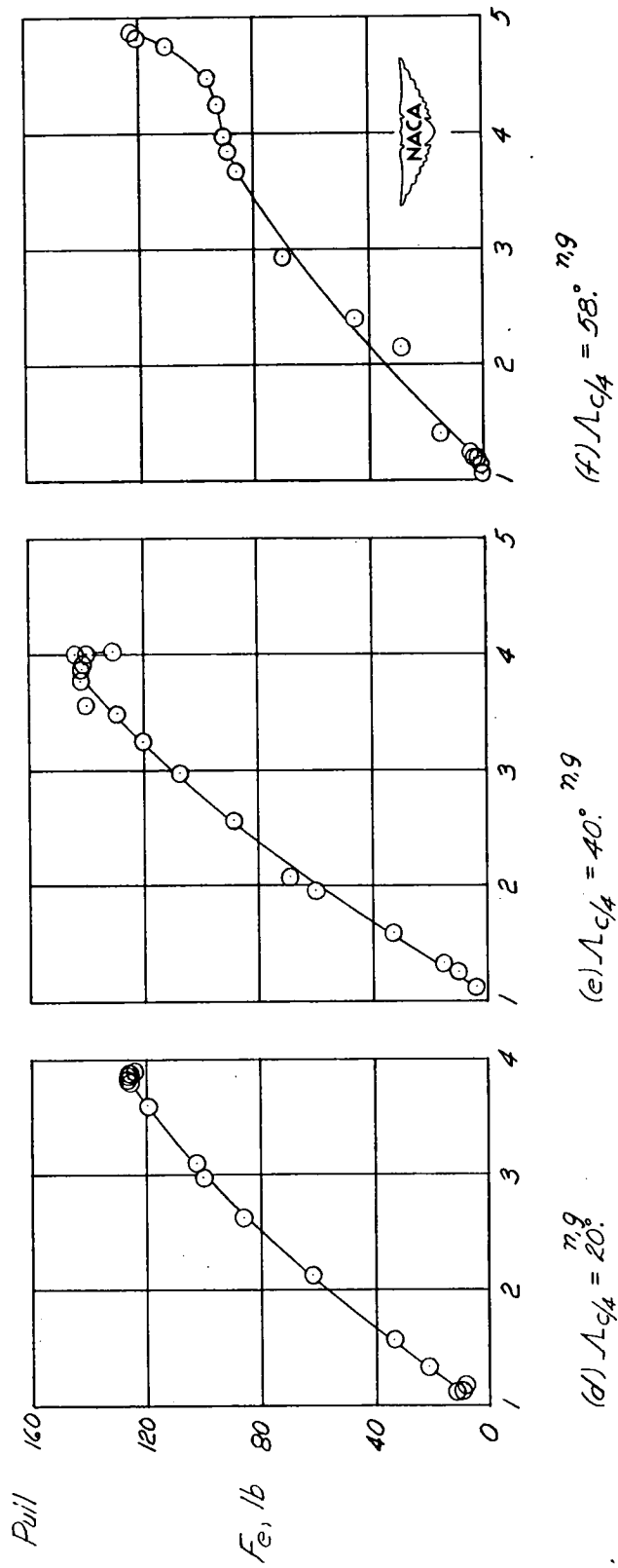


Figure 12.- Concluded.

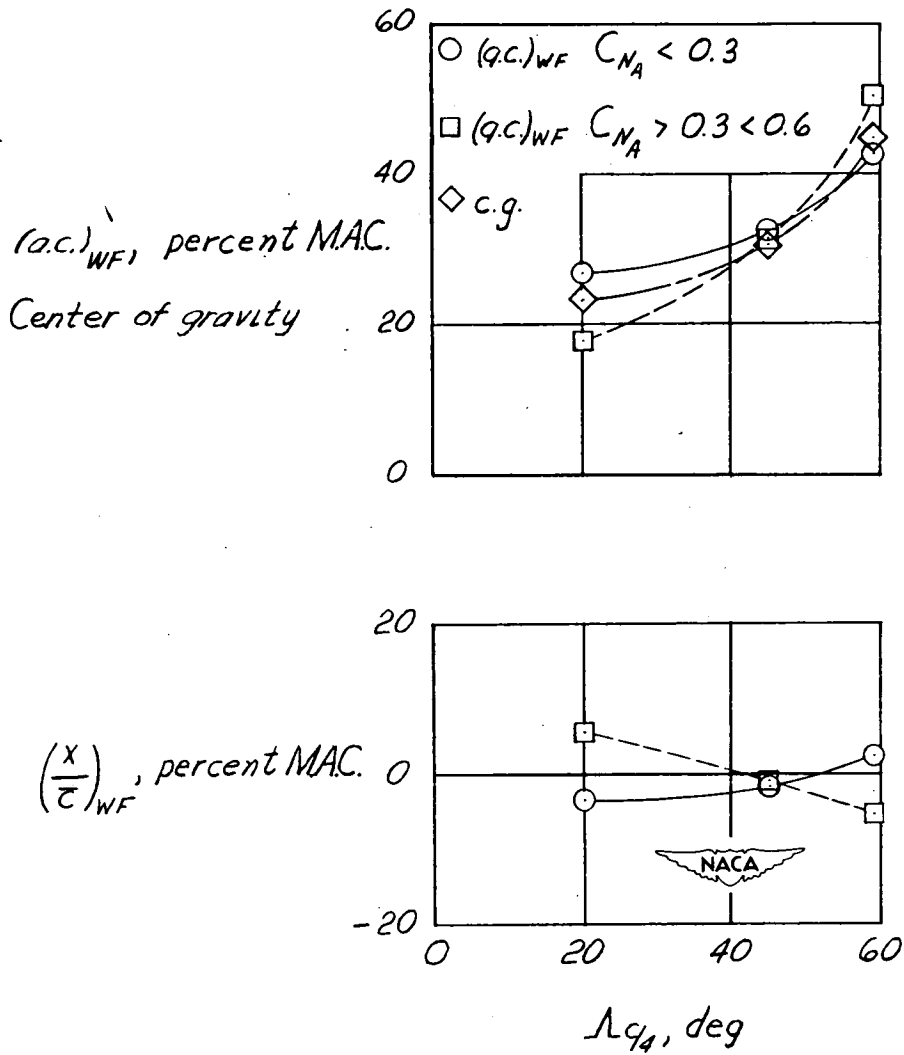


Figure 13.- Variation of aerodynamic center and static margin of the wing-fuselage combination and the airplane center of gravity with wing sweep angle at  $M \approx 0.83$ .

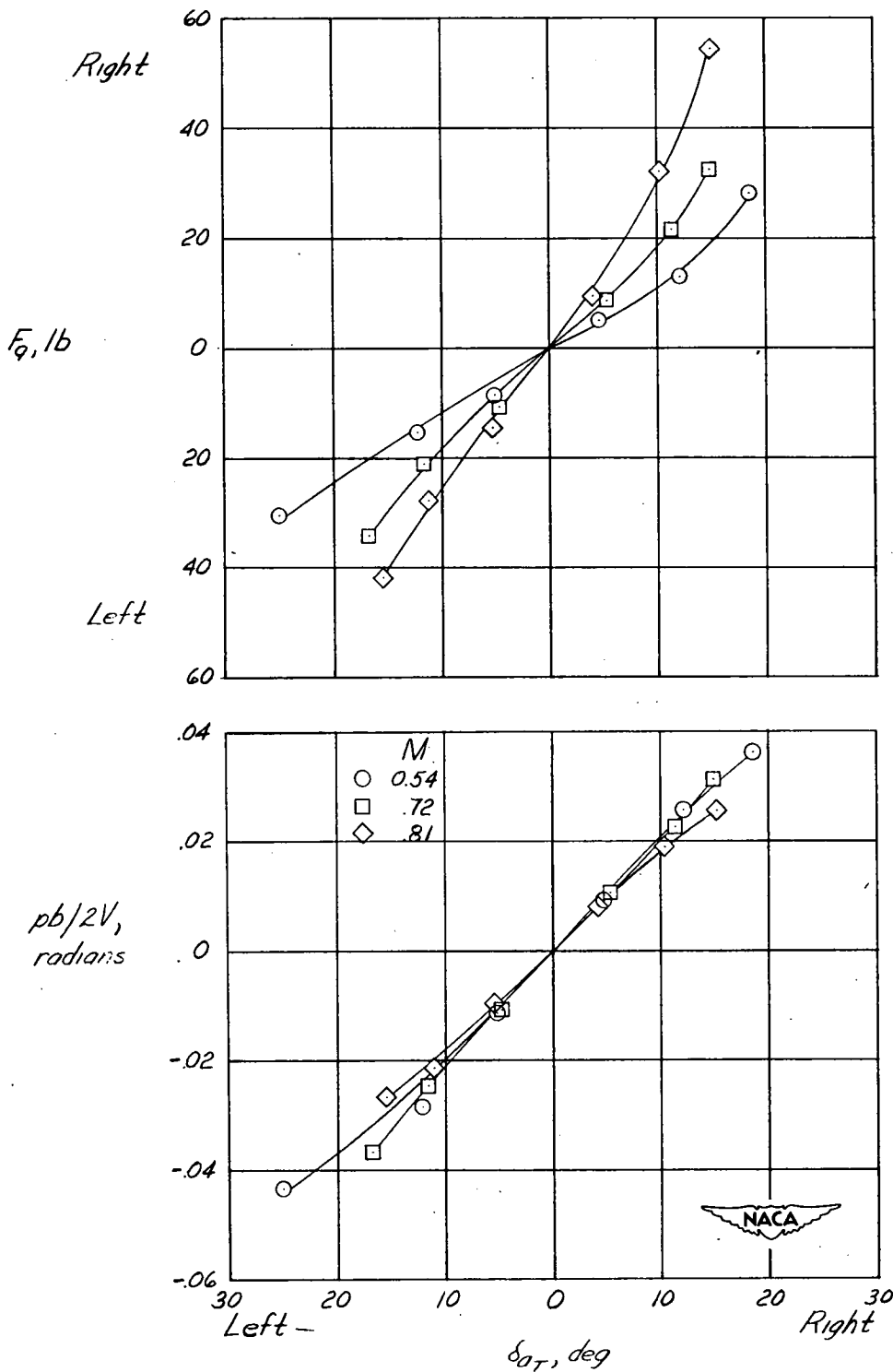


Figure 14.- Variation of aileron stick force and wing-tip helix angle with total aileron deflection in the clean configuration for Mach numbers of 0.54, 0.72, and 0.81 at 20° sweepback.  $h_p = 25,000$  feet.

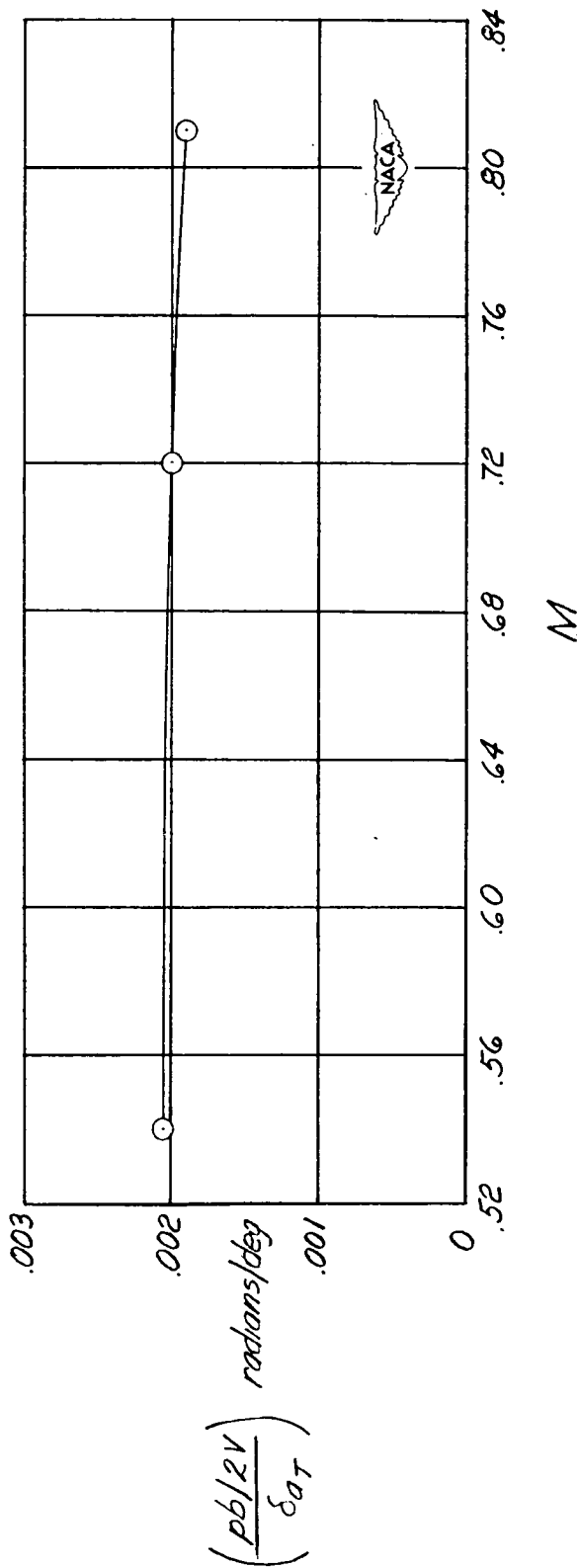


Figure 15.- Variation of wing-tip helix angle per degree of total aileron deflection with Mach number in the clean configuration for total aileron deflections of  $\pm 10^\circ$ .  $h_p = 25,000$  feet;  $\Lambda_c/4 = 20^\circ$ .

$$\left( \frac{pb/2V}{\delta_{aT}} \right)$$